Field Observations of Surf Zone–Inner Shelf Exchange on a Rip-Channeled Beach

JENNA A. BROWN AND JAMIE H. MACMAHAN

Department of Oceanography, Naval Postgraduate School, Monterey, California

AD J. H. M. RENIERS

Department of Hydraulic Engineering, Delft University of Technology, Netherlands

ED B. THORNTON

Department of Oceanography, Naval Postgraduate School, Monterey, California

(Manuscript received 19 June 2014, in final form 5 June 2015)

ABSTRACT

Cross-shore exchange between the surf zone and the inner shelf is investigated using Lagrangian and Eulerian field measurements of rip current flows on a rip-channeled beach in Sand City, California. Surface drifters released on the inner shelf during weak wind conditions moved seaward due to rip current pulses and then returned shoreward in an arcing pattern, reentering the surf zone over shoals. The cross-shore velocities of the seaward- and shoreward-moving drifters were approximately equal in magnitude and decreased as a function of distance offshore. The drifters carried seaward by the rip current had maximum cross-shore velocities as they exited the surf zone and then decelerated as they moved offshore. The drifters moving shoreward accelerated as they approached the surfzone boundary with maximum cross-shore velocities as they reentered the surf zone over shoals. It was found that Stokes drift was not solely responsible for the onshore transport across the surfzone boundary. The cross-shore diffusivity on the inner shelf was greatest during observations of locally contained cross-shore exchange. These field observations provide evidence that the cross-shore exchange between the surf zone and inner shelf on a rip-channeled beach is due to wave-driven rip current circulations and results in surface material being contained within the nearshore region.

1. Introduction

The cross-shore exchange of material across the surfzone boundary, in both the seaward and shoreward directions, plays an important role in processes ranging from how land-based pollution, which enters the ocean in the surf zone (e.g., Schiff et al. 2000; Boehm et al. 2002), is carried offshore to the inner shelf, to how harmful algae blooms and offshore operational discharges, such as oil, which originate in the inner shelf, are transported into the surf zone (e.g., Anderson 2009; Michel et al. 2013). Understanding the transport and retention of hazardous pollutants and biological matter in the nearshore region is important for reasons ranging from human health factors to sustaining ecosystems (e.g., Shahidul Islam and Tanaka 2004; Grant et al. 2005).

Studies of cross-shore circulation over the inner shelf, focusing on wave-driven flows (i.e., during weak wind forcing), demonstrate the importance of the onshore Lagrangian Stokes drift $u_{St}(z)$ associated with shoreward-propagating surface gravity waves (Stokes 1847). A compensating wave-driven offshore Eulerian flow $u_E(z)$ exists below the wave trough, referred to as undertow. The presence of wave-driven Eulerian undertow inside the surf zone is widely known and has been measured extensively in the field (Haines and Sallenger 1994; Garcez Faria et al. 2000; Reniers et al. 2004b) and has also been found to extend well offshore on the inner shelf (Lentz et al. 2008; Kirincich et al. 2009; Ohlmann et al. 2012). The summation of $u_{St}(z)$ and $u_E(z)$, throughout the water column at a given location, results in a wave-averaged Lagrangian velocity $u_L(z)$, where z is the vertical elevation defined as positive upward from the sea surface.

Corresponding author address: Jenna A. Brown, U.S. Geological Survey, St. Petersburg Coastal and Marine Science Center, 600 4th St. S, St. Petersburg, FL 33701.
E-mail: jennabrown@usgs.gov

DOI: 10.1175/JPO-D-14-0118.1

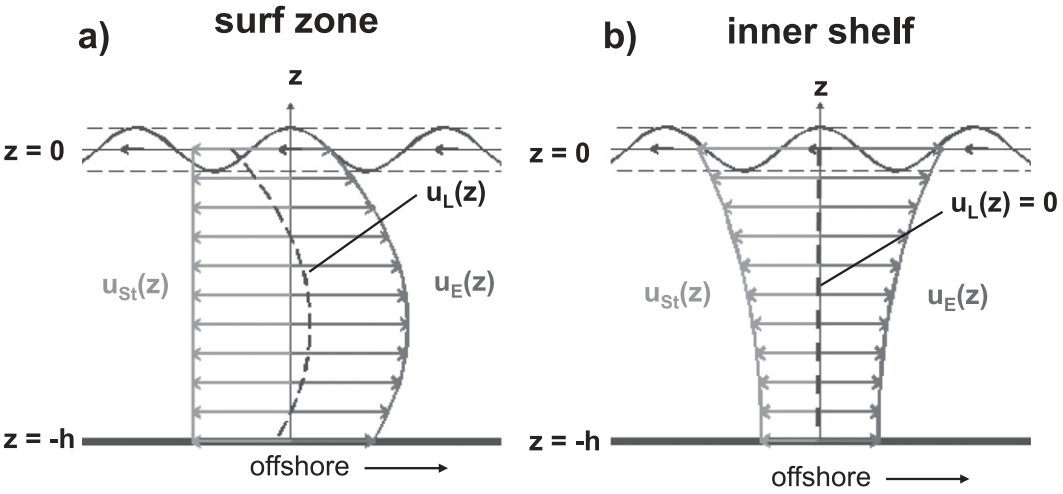

FIG. 1. Two-dimensional (x, z) wave-driven circulation typically observed (a) inside the surf zone where the onshore Lagrangian Stokes drift $u_{St}(z)$ is uniform in depth and the offshore wave-driven Eulerian undertow $u_E(z)$ is parabolic resulting in a vertical imbalance and $u_L(z) \neq 0$ (dashed line), and (b) over the inner shelf, where the onshore Lagrangian Stokes drift $u_{St}(z)$ and the offshore wave-driven Eulerian undertow $u_E(z)$ cancel, resulting in a vertical balance and net Lagrangian velocity $u_L(z) = 0$ (dashed line) at all depths. The black wavy line represents the instantaneous sea surface.

Inside the surf zone, current dynamics are predominantly driven by breaking surface gravity waves and are largely dependent on the surfzone bathymetry. In a surf zone characterized by an alongshore homogeneous morphology, the onshore Stokes drift profile is vertically uniform, and the Eulerian undertow flow has a parabolic velocity profile with maximum offshore velocity at middepth or near bottom (Svendsen 1984; Putrevu and Svendsen 1993; Haines and Sallenger 1994; Garcez Faria et al. 2000; Reniers et al. 2004b), resulting in an imbalance between $u_{St}(z)$ and $u_E(z)$ throughout the water column (Fig. 1a).

Outside the surf zone in deep water, the onshore Stokes drift is largest at the surface and decays exponentially with depth. On the inner shelf of Martha's Vineyard, Massachusetts, and Duck, North Carolina, during weak wind conditions and along-shelf uniform flows, Lentz et al. (2008) found that the wave-driven Eulerian undertow profile was distributed as predicted by Hasselmann with maximum offshore flow at the surface and decreasing toward the bottom (Hasselmann 1970). This resulted in a vertical balance between $u_{St}(z)$ and $u_E(z)$, so $u_L(z)$ is zero at all depths and there is a zero net Langrangian transport (Fig. 1b) (Hasselmann 1970; Xu and Bowen 1994; Smith 2006; Monismith et al. 2007; Lentz et al. 2008; Hendrickson and MacMahan 2009). Expanding upon these findings, Ohlmann et al. (2012) released drifters during weak wind conditions on the inner shelf off the coast of two beaches in southern California that are relatively alongshore uniform and typically do not support rip currents. A deceleration of shoreward-moving surface drifters was observed, which was attributed to an imbalance of $u_{St}(z)$ and $u_E(z)$ near the surfzone boundary resulting in a net offshore Langrangian flow near the water surface. The results of Ohlmann et al. (2012) suggest that surface waves drive offshore Eulerian flows in the upper water column that may prevent the onshore transport of material into the surf zone from the inner shelf.

These findings of cross-shore transport over the inner shelf on relatively alongshore homogeneous beaches are used as a starting point to investigate cross-shore exchange on rip-channeled beaches. Rip currents commonly occur in some variation on most sandy beaches and have been observed in nature and studied extensively for many years (e.g., Shepard et al. 1941; Bowen 1969; Smith and Largier 1995; Brander and Short 2001; MacMahan et al. 2005, 2006; among others). Rip currents are strong, seaward-directed flows that originate near the shoreline and have long been believed to extend well beyond the surf zone and wave breaking and thereby are a means of continuously transporting material offshore (Shepard et al. 1941; Inman and Brush 1973). Bathymetrically controlled rip currents are coupled to the underlying beach bathymetry, characterized by deeper, incised channels in shallower, shore-connected shoals or alongshore bars and are the focus of the work presented here. Additionally, transient rip currents have been observed on alongshore homogeneous beaches (Johnson and Pattiaratchi 2004; MacMahan et al. 2010b;

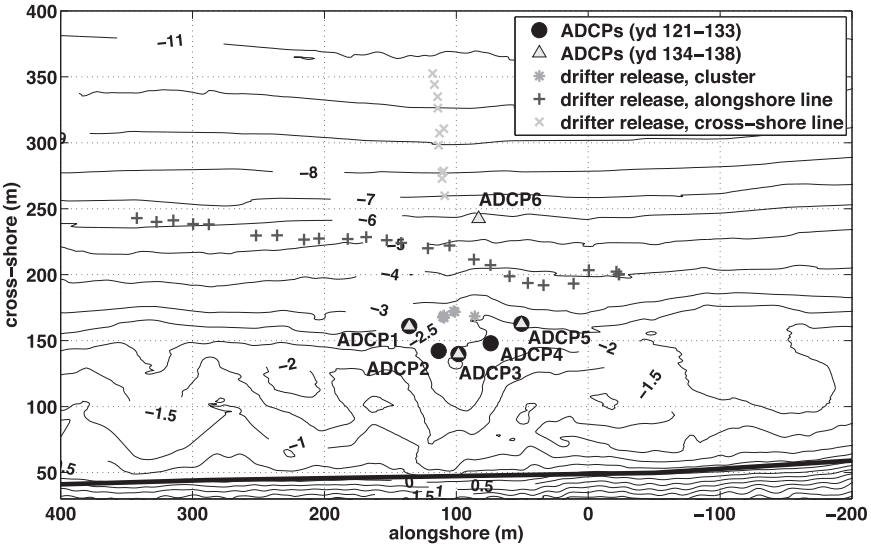

FIG. 2. Field experiment site in the local coordinate system, where the thin black lines are the bathymetry contours (labeled with the elevation in meters relative to MSL), and the thick black line represents the mean shoreline. In situ ADCP locations are shown, where black circles are the locations for yeardays 121 to 133 and gray triangles are the locations for yeardays 134 to 138. Examples of the three drifter release approaches are shown from yearday 130: 1) in a cluster at the offshore edge of a rip channel, just outside the surf zone (* symbols); 2) in an alongshore line outside the surf zone, spanning multiple shoals and rip channels (+ symbols); and 3) in a cross-shore line outside the surf zone, in line with a rip channel (x symbols).

Hally-Rosendahl et al. 2014), which occur spontaneously because of the interaction of vortices generated in the surf zone by wave groups (Reniers et al. 2004a) or by short-crested wave breaking (Clark et al. 2012), and eject material seaward. Recently, MacMahan et al. (2010a) deployed a fleet of position-tracking surface drifters in different open coast beach rip current systems and observed rip current flow patterns composed of semi-enclosed, large-scale vortices that were contained within the surf zone and largely retained drifters (only 17% drifter exits per hour). Rip current surfzone retention and exchange evaluated with a three-dimensional (3D) numerical model demonstrated the importance of including Stokes drift and very low-frequency (VLF) motions to accurately describe the behavior of rip current exits (Reniers et al. 2009, 2010), where excluding either term resulted in an over or under estimation, respectively, of drifter exits (Reniers et al. 2009). Smith and Largier (1995) observed rip currents that episodically transported water offshore with a sector-scanning Doppler sonar in La Jolla, California, and concluded that rip currents could cause significant cross-shore exchange, capable of flushing the surf zone in roughly 3 h. These studies demonstrate the ability of rip currents to transport material offshore. However, it still remains largely unknown how rip currents act as a transport mechanism, both temporally and spatially, between the surf zone and the inner shelf.

In this work, an extensive set of Lagrangian and Eulerian field measurements of rip current flows on the inner shelf is analyzed to evaluate cross-shore exchange on a rip-channeled beach in Sand City, California. The observations are unique in that they describe flows outside of the surf zone and the fate of material transported offshore via rip currents, which have not been extensively measured before on a rip-channeled beach. The results of these observations are presented and comparisons to studies of cross-shore exchange on alongshore homogeneous beaches are discussed.

2. Field experiment

a. Field site and wave, wind, and tide measurements

The exchange of material between the surf zone and the inner shelf was examined on a rip-channeled beach at Sand City, California, in southern Monterey Bay in May 2009. Bathymetry, offshore waves, wind, tidal elevation, and currents were measured throughout the field experiment. The beach is composed of a 1/10 sloping foreshore with straight and parallel contours, flattening out to a 1/100 slope inshore with quasi periodic, $O(125)$ m, incised rip channels and continuing with a 1/20 offshore slope with straight and parallel contours seaward of the breaker zone (Fig. 2). Routine bathymetric surveys

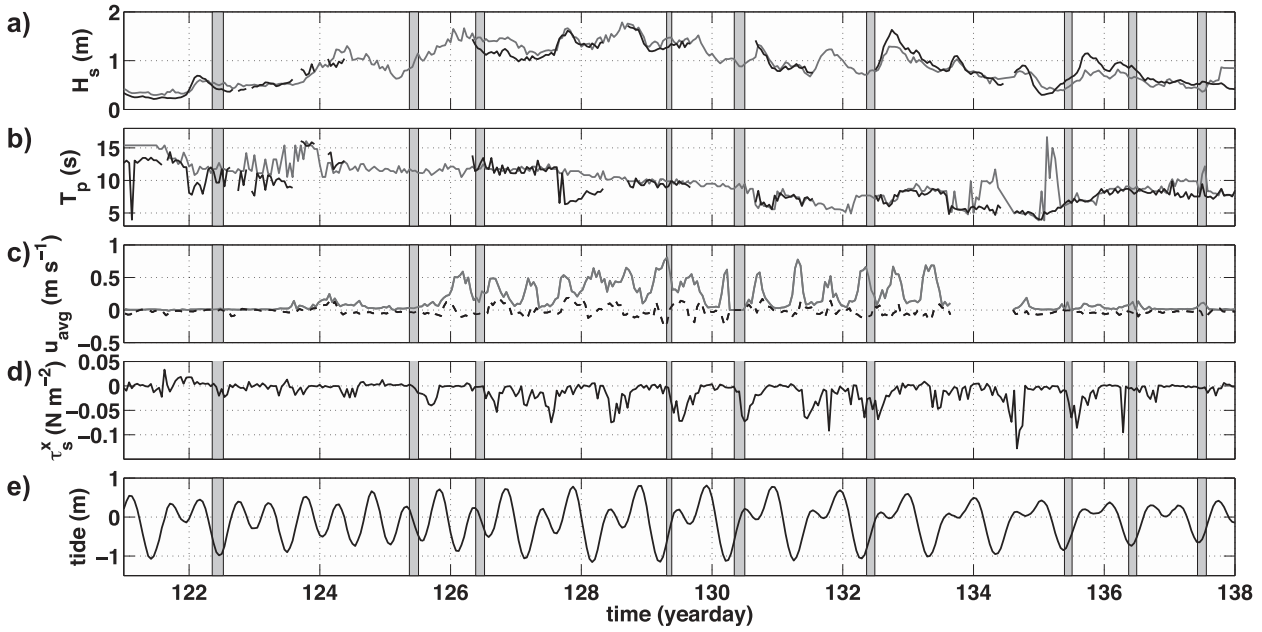

FIG. 3. Conditions measured during the field experiment of hourly mean (a) significant wave height H_s; (b) peak wave period T_p; (c) depth-averaged cross-shore (solid line) and alongshore (dashed line) velocities measured by ADCP 3 in the rip channel; (d) onshore wind stress τ_s^x; and (e) tidal elevation relative to MSL. In (a) and (b) the black lines are measured by the ADCP in 13-m water depth, and gray lines are measured by NDBC buoy 46240 shoaled to 13-m water depth. Gray shaded regions represent times of drifter deployments.

were performed using a kinematic global positioning system (GPS) device mounted to a sonar-equipped personal watercraft (MacMahan 2001) and a GPS-equipped walking person. The local coordinate system used in this work is defined as cross-shore coordinate x increasing positively offshore and alongshore coordinate y increasing positively to the south.

Offshore waves were measured in 13-m water depth with an acoustic Doppler current profiler (ADCP) and were hourly averaged (Fig. 3). Gaps in the offshore ADCP wave data occurred because of instrument fouling and during these times waves measured by National Data Buoy Center (NDBC) buoy 46240, located in 18.5-m water depth and just south of the field site, were shoaled to 13 m using linear wave theory (Dean and Dalrymple 1984) and were hourly averaged (Fig. 3, gray lines). Hourly mean wind speed and direction were recorded atop a 10-m tower onshore of the field site and rotated to the local coordinate system, and wind stress was calculated using the method by Large and Pond (1981) (Fig. 3). Hourly mean tidal elevation was obtained from the nearby National Ocean Service (NOS) tidal station 9413450 (Fig. 3).

To estimate the surfzone width L_x, the mean offshore wave conditions were shoaled using linear wave theory (Dean and Dalrymple 1984) to the shoreline using the alongshore-averaged cross-shore beach profile, adjusted for the tidal elevation, with a depth-limited wave-breaking criterion of $H_s/h \geq 0.4$ (Thornton and Guza 1982). The cross-shore location of the surfzone boundary X_{sz} is defined as the cross-shore location of the maximum significant wave height H_s, and the cross-shore location of the shoreline X_{sh} is defined as the cross-shore location where the water depth h, adjusted for the tidal elevation, is zero, with the surfzone width $L_x = X_{sz} - X_{sh}$. Throughout this work, cross-shore extents are given as distance from the shoreline $X = x - X_{sh}$ relative to the surfzone width, where $X/L_x = 1$ represents the edge of the surf zone.

b. *Eulerian current measurements*

Five ADCPs were deployed to obtain in situ Eulerian current and pressure measurements for 17 days in an alongshore array on the 2.5-m depth contour at the approximate offshore edge of the surf zone (Fig. 2). ADCPs 1, 2, 3, and 4 sampled at $dt = 2$ s with a measurement bin size of 0.11 m, and ADCP 5 sampled at $dt = 3$ s with a measurement bin size of 0.25 m. For the last 4 days of the experiment (yeardays 134 to 138), one ADCP was moved offshore (labeled ADCP 6), in line with a rip channel in the surf zone, to measure inner shelf flows, and three ADCPs remained in the alongshore array (Fig. 2). During this time, ADCPs 1, 3, and 6 sampled at $dt = 1$ s with a measurement bin size of

TABLE 1. Summary of conditions observed during the drifter deployments, grouped by observed drifter pattern. Tidal elevation was obtained from NOS tidal station 9413450; wave parameters and surfzone characteristics were obtained from the offshore ADCP in 13-m water depth when data were available and otherwise were obtained from NDBC buoy 46240; wind data were recorded atop a 10-m tower onshore of the field site; depth-averaged cross-shore velocity u_{avg} was measured by ADCP3, and alongshore velocity v_{avg} was computed from the drifters; and cross-shore location of the surfzone boundary X_{sz} and surfzone width L_x were determined by shoaling waves from the ADCP in 13-m water depth to the shoreline using linear wave theory. The asterisk indicates that the sensor was buried.

Yearday	Drifter pattern/ exchange type	Tidal elevation (m)	H_s (m)	T_p (s)	τ_s^x (N m^{-2})	u_{avg} (m s^{-1})	v_{avg} (m s^{-1})	X_{sz} (m)	L_x (m)	Maximum drifter cross-shore extent (X/L_x)
122	Cross-shore	−0.87	0.43	10.6	−0.01	0.01	0.05	147	78	3.6
129	Cross-shore	−0.30	1.31	9.5	−0.02	0.70	0.00	180	123	3.8
132	Cross-shore	−0.51	0.77	7.6	−0.03	0.35	−0.04	157	97	3.7
125	Cross-shore and alongshore	−0.14	0.97	11.5	−0.01	0.03	−0.14	176	122	1.9
126	Cross-shore and alongshore	−0.05	1.22	12.6	0.00	0.20	−0.15	174	122	2.8
130	Cross-shore and alongshore	−0.02	0.92	9.2	−0.04	—*	0.13	162	111	3.3
137	Cross-shore and alongshore	−0.54	0.55	8.2	−0.01	0.08	0.13	142	81	2.5

0.10 m, and ADCP 5 sampled at $dt = 3$ s with a measurement bin size of 0.25 m. Sea surface elevations, including variations due to short ($0.04 < f < 0.25$ Hz) waves, were computed from the ADCP pressure sensor measurements, and ADCP velocities that occurred above the sea surface elevation were removed. Owing to variations of the instantaneous sea surface elevation with time, velocities above the MSL were retained. The hourly mean, depth-averaged cross-shore and alongshore velocities, u_{avg} and v_{avg}, respectively, measured by the ADCP in the primary rip channel (ADCP 3: $x = 140$ m, $y = 100$ m) are shown in Fig. 3, and the depth-averaged cross-shore velocity averaged over the duration of each drifter deployment is given in Table 1.

c. *Lagrangian drifter deployments*

A fleet of Lagrangian surfzone drifters equipped with GPS devices was deployed to measure surface current patterns outside the surf zone. See MacMahan et al. (2009) for a complete description of the drifter design and performance. The drifter positions, sampled every 2 s, were converted to the local coordinate system and filtered to remove erroneous points. Velocity estimates were computed using a forward-differencing scheme. Seven drifter deployments were conducted during varying wave and tidal conditions, each lasting approximately 3 h with between 28 to 45 drifters being released. In an attempt to capture the spatial variation of rip current flows that exit the surf zone, drifters were released using three approaches: 1) by swimmers in a cluster at the offshore edge of a rip channel, just outside of the surf zone (Fig. 2, * symbols); 2) by a boat in an alongshore line just outside of the surf zone, spanning 4–5 rip channel–shoal systems (Fig. 2, + symbols); and 3) by a boat in a cross-shore line spanning from the edge of the surf zone and extending up to two surfzone widths offshore, in line with a rip channel (Fig. 2, x symbols). Conditions during the drifter deployments consisted of offshore waves with significant wave heights H_s of 0.43 to 1.31 m, peak wave periods T_p of 7.6 to 12.6 s, onshore wind stress τ_s^x less than 0.04 N m^{-2}, and L_x of 78 to 123 m (Table 1). All drifter deployments occurred during low tides (tidal elevation < MSL), to ensure rip current flows would be induced by the rip-channeled morphology, and during weak wind conditions, defined as $\tau_s^x < 0.05$ N m^{-2} by Ohlmann et al. (2012), allowing for the wave-driven transport to be examined separately. The wind slippage of the drifters was assumed to be weak (maximum biased error of 0.04 m s^{-1}), and onshore wind was not considered a factor in the drifters (Table 1).

3. Lagrangian observations

a. *Qualitative drifter patterns*

In general, the drifters released outside the surf zone initially moved seaward because of the rip currents, typically reaching a maximum cross-shore extent of $3L_x$ and eventually returned shoreward in an arcing pattern, at times reentering the surf zone over shoals, with no drifters being permanently removed from the nearshore region. The qualitative drifter observations support the numerical modeling results of Reniers et al. (2010), which showed that Lagrangian coherent structures (LCSs) in the rip current flows had offshore limits prohibiting further cross-shore transport and resulting in the shoreward return of drifters. Results from each

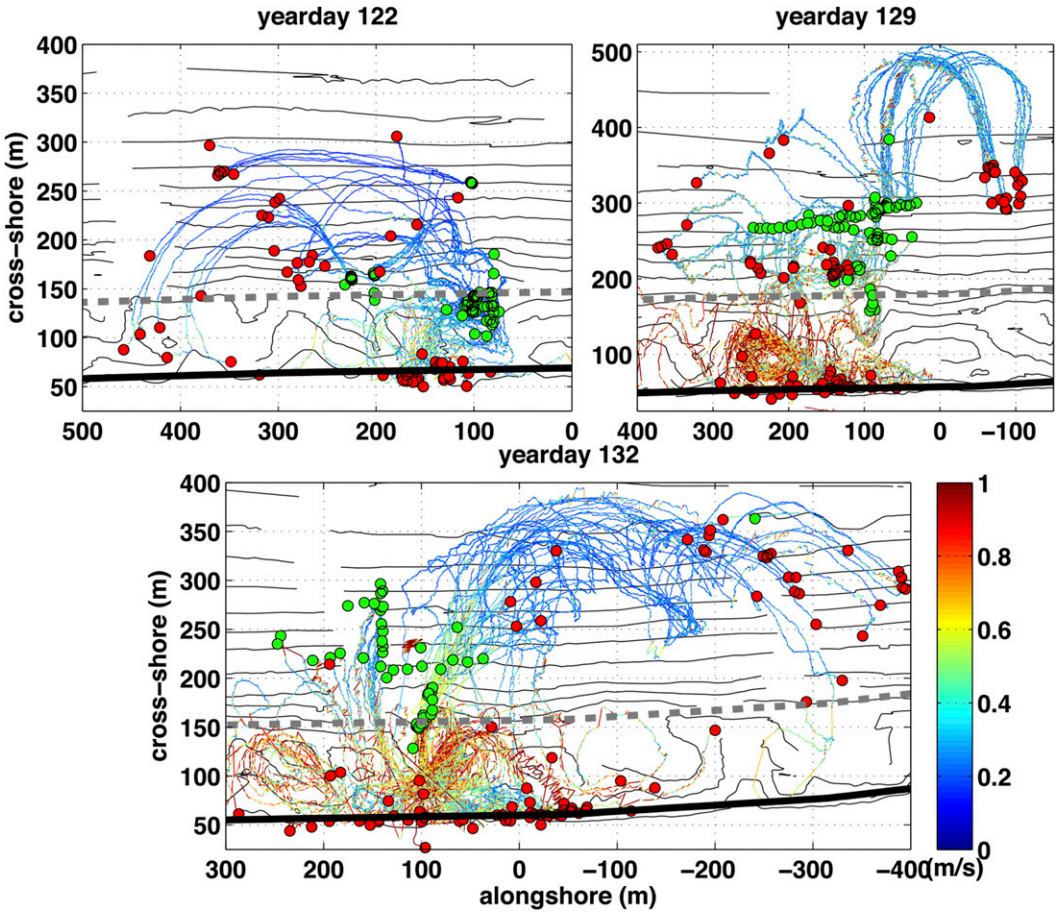

FIG. 4. Drifter positions and speed, where the color of the line represents the speed, for drifter deployments exhibiting the locally contained cross-shore exchange drifter pattern on yeardays 122, 129, and 132. Bathymetry contours are shown in the background in black, the shoreline X_{sh} is shown as the thick black line, and the approximate surfzone boundary X_{sz} is shown as the dashed gray line. Color bar represents the drifter speed. Green circles show drifter release locations, and red circles show drifter retrieval locations. Note there are different cross-shore and alongshore scales between plots.

individual drifter deployment are shown in Figs. 4 and 5, where the track of every drifter that was released during the deployment is plotted, and the color of the track represents the speed of the drifter. Two distinguishable drifter patterns were observed on the inner shelf: 1) the drifters moved seaward and returned sharply back shoreward a short alongshore distance from where they exited, resulting in cross-shore exchange that was locally contained (Fig. 4), and 2) the drifters moved seaward and traveled farther in the alongshore direction as they gradually moved shoreward, resulting in cross-shore and alongshore exchange (Fig. 5).

1) LOCALLY CONTAINED CROSS-SHORE EXCHANGE

The locally contained cross-shore exchange pattern was observed on yeardays 122, 129, and 132, when the rip currents were stronger during low tides and the alongshore currents outside the surf zone were weak (indicated by small mean alongshore drifter velocities outside the surf zone, as shown in Table 1). On yearday 122 (Fig. 4), clusters of drifters released at the edge of the surf zone ($X = 1L_x$) and at about $X = 2.5L_x$, offshore of the primary rip channel ($y = 100$ m), tended to move seaward and to the south, moving back shoreward and reentering the surf zone over shoals less than 350 m down the beach. The maximum extent of all drifters regardless of cross-shore release location was approximately the same and was $3.6L_x$. At different times during the deployment, drifters were observed to move shoreward and seaward at approximately the same location offshore of a rip channel ($y = 250$ m, $x = 200$ m), depending on if the rip current was pulsing or not at that time.

On yearday 129 (Fig. 4), the first drifter release occurred just after low tide, with a total of 27 drifters being

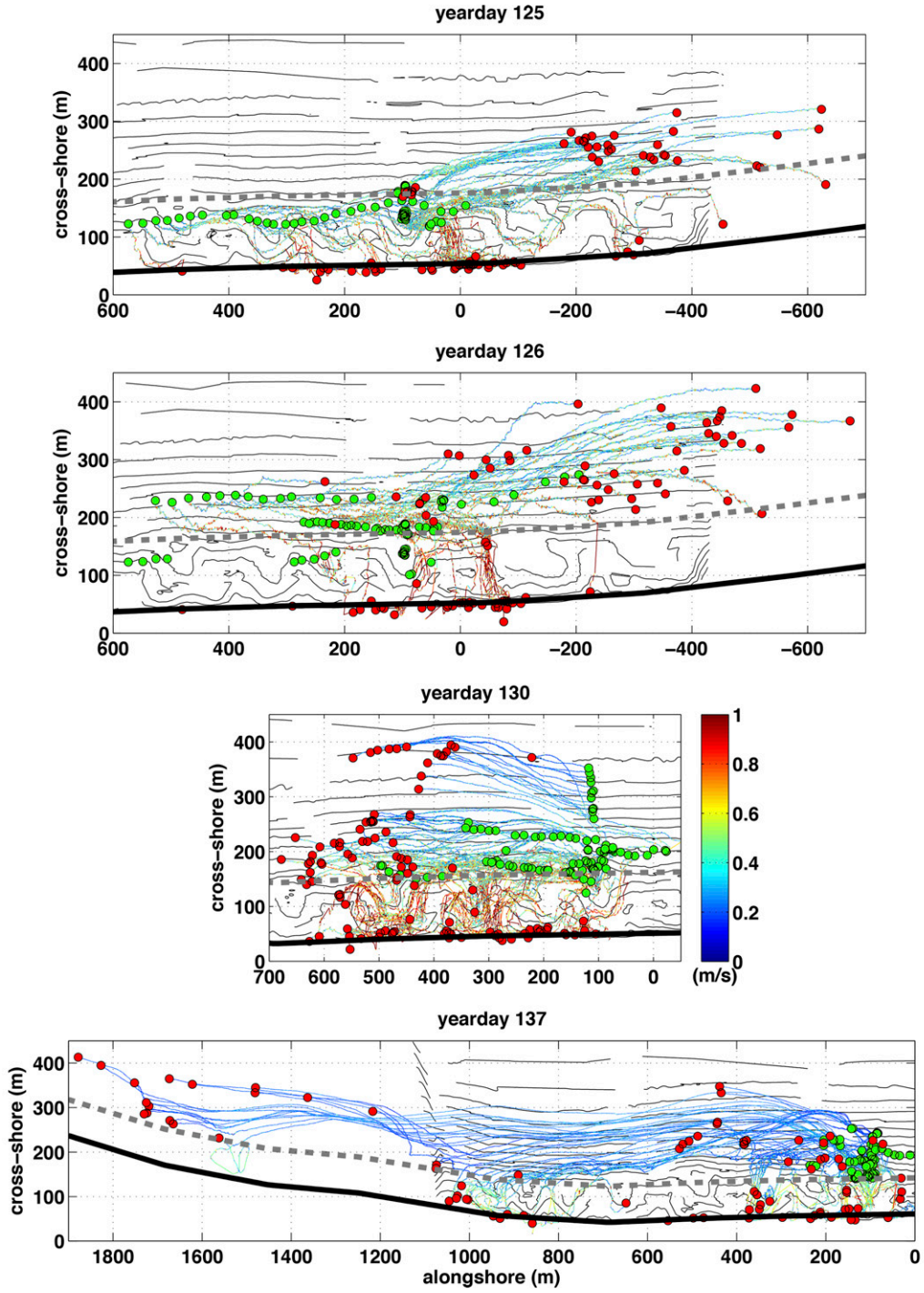

FIG. 5. As in Fig. 4, but for drifter deployments exhibiting the cross-shore and alongshore exchange drifter pattern on yeardays 125, 126, 130, and 137.

released in an alongshore line at approximately $X = 1.8L_x$, spanning the width of two rip channels and two shoals. In general, drifters that were released to the south of the primary rip channel ($y > 100$ m) moved directly shoreward and entered the surf zone over a shoal. Drifters that were released offshore of the primary rip channel and to the north ($y \leq 100$ m) moved seaward about 200 m farther, reaching a maximum cross-shore extent of $X = 3.8L_x$ and then typically turned north, arcing sharply, and moved back shoreward

within 200 m or less in the alongshore direction from where they initially moved seaward. Another alongshore line of drifters was released 2 h after the initial release at approximately the same cross-shore location, and all of these drifters moved shoreward, most likely due to the rising tide and the weakening of the rip current.

Similar results were seen on yearday 132 (Fig. 4), where drifters released offshore of shoals moved directly shoreward, entering the surf zone over the shoal. Drifters released offshore of the primary rip channel ($y = 100$ m) moved seaward and to the north and returned shoreward within 300 m in the alongshore direction of their release location. Interestingly, all of these drifters were pushed back offshore when they reached $y = -100$ to -200 m (offshore of a rip channel) because of a neighboring pulsing rip current. The drifters again moved seaward and north, and then returned shoreward within 200 m or less in the alongshore direction. The maximum offshore extent of the drifters on this day was $3.7L_x$.

2) Cross-shore and alongshore exchange

The cross-shore and alongshore exchange pattern was observed on yeardays 125, 126, 130, and 137, when the rip currents were weak during higher tidal elevations and the alongshore current outside the surf zone was stronger (Table 1). On yearday 125 (Fig. 5), the first drifter release consisted of 29 drifters being released in an alongshore line, approximately 20 m apart, spanning an alongshore distance of about 600 m and encompassing five shoals and four rip channels. The surf zone was relatively wide ($L_x = 122$ m) so the alongshore line was actually inside of the surf zone. Drifters released to the south of the primary rip channel ($y > 100$ m) meandered alongshore to the north inside the surf zone, following the underlying bathymetry contours. A number of these drifters ended up on the beach, and others were pushed seaward because of the rip current at $y = 100$ m. The drifters released near the primary rip channel and to the north ($y < 100$ m) moved seaward and to the north. The drifters that were outside of the surf zone continued to move seaward and to the north and then gradually moved back shoreward, with some being pushed back offshore because of the rip currents to the north. These drifters were picked up before they could reenter the surf zone. which was 500 to 700 m alongshore to the north from where they exited the surf zone. The cross-shore extent of the drifters on this day was within $2L_x$. Additional clusters of drifters were released in the primary rip channel near the offshore edge of the surf zone, and these all moved in a similar pattern seaward and to the north. A similar drifter pattern was observed on yearday 126 (Fig. 5). Again, an alongshore line of drifters was released, this time just outside of the surf zone, and the drifters either moved into the surf zone or alongshore and were eventually pushed seaward and to the north. The cross-shore extent was about $2.8L_x$, and again the drifters were picked up greater than 600 m to the north from where they were pushed seaward as they were beginning to gradually move shoreward.

On yearday 130 (Fig. 5), in general, drifters that were released outside of the surf zone and offshore of the primary rip channel or to the north ($y < 100$ m) were pushed seaward as they moved alongshore to the south and then began moving shoreward once they were about 300 m to the south of the rip channel ($y = 400$ m). Drifters that were released outside of the surf zone and to the south of the primary rip channel ($y > 100$ m) moved predominantly alongshore with little to no seaward movement and gradually moved shoreward. The cross-shore extent of the rip current was demonstrated by a release of drifters in a cross-shore array offshore of the primary rip channel, spanning approximately $X = 1.5L_x$ to $X = 2.5L_x$, where all of the drifters moved south and seaward and seemed to converge at a cross-shore extent of about $3.3L_x$, where they then began moving shoreward. Drifters that were released at the surfzone boundary were immediately pulled into the surf zone over a shoal. As the tide rose during the deployment, the rip current weakened and no drifters moved seaward, and the drifters inside of the surf zone exhibited a meandering current pattern. Throughout the deployment, all drifters that moved seaward and alongshore outside of the surf zone were picked up 300 to 500 m south of the primary rip channel, before they had a chance to reenter the surf zone, indicating a significant amount of alongshore transport was occurring.

The drifter deployment on yearday 137 (Fig. 5) occurred during low tide with relatively small wave conditions, resulting in a narrow surf zone ($L_x = 81$ m). Drifters were released in a cross-shore array in line with the primary rip channel between 1 and $2L_x$. The rip current pulse pushed the drifters seaward and to the south, with a maximum cross-shore extent of about $2.5L_x$. A number of the drifters gradually returned shoreward and approached the surfzone boundary greater than 500 m from where they were released, with many of the drifters then being pushed back offshore and to the south exhibiting a meandering alongshore current pattern outside of the surf zone within $2L_x$. Shear in the alongshore current outside of the surf zone can be seen in the drifter results, with the alongshore current magnitude decreasing near the surfzone boundary.

b. Drifter one-particle diffusivity statistics on the inner shelf

The movements of the drifters outside the surf zone were evaluated using one-particle statistics, which describe the average drifter evolution from a common

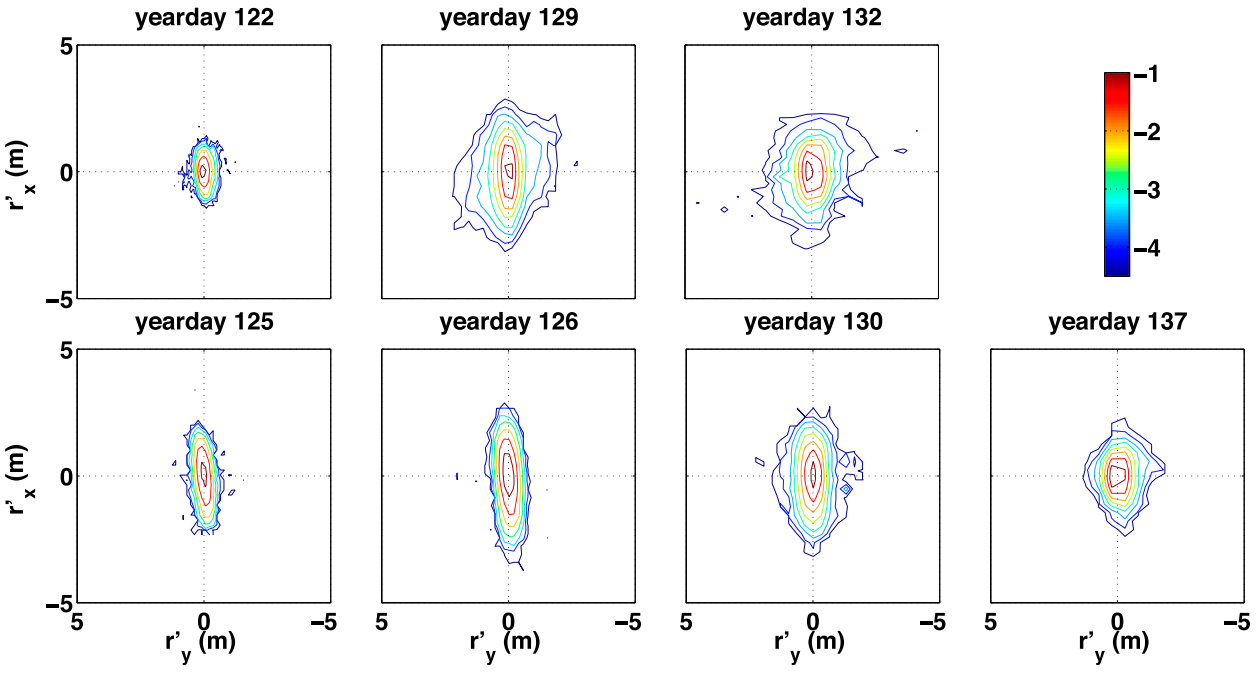

FIG. 6. Log–log plots of the pdf of the anomalous relative drifter position displacements outside the surf zone for a relative time step of $t' = 2$ s for (top) drifter deployments exhibiting the locally contained cross-shore exchange drifter pattern on yeardays 122, 129, and 132 and (bottom) drifter deployments exhibiting the cross-shore and alongshore exchange drifter pattern on yeardays 125, 126, 130, and 137. Contours are $\log_{10}[P(r'_x, r'_y; t' = 2\,\text{s})] = -4.5, -4, -3.5, \ldots, -1.5, -1$.

release point. The trajectories of the drifters are represented as the collection of relative position displacements, $\mathbf{r}(t') = \mathbf{x}(t'_0 + t') - \mathbf{x}(t'_0)$, for a relative time step t', computed as the difference between the drifter position, $\mathbf{x} = (x, y)$ at an earlier time t'_0 from the position a time t' later. Each recorded drifter position is considered a possible starting position $\mathbf{x}(t'_0)$. Therefore, a drifter time series with N total position measurements yields $(N - 1)$ values for $\mathbf{r}(t' = 2\,\text{s})$ (Spydell et al. 2007). All drifters released during a given deployment can be viewed as originating from a common release point, and the random motions represented by the drifter trajectories can be described in the same manner as bulk molecular diffusion (Taylor 1922). The one-particle absolute diffusivity κ_{ij} is related to the change in drifter displacement variance σ^2_{ij} with time:

$$\kappa_{ij}(t') = \frac{1}{2}\frac{d}{dt'}\sigma^2_{ij}(t'), \tag{1}$$

where $i, j = x, y$, and σ^2_{ij} is the second moment of displacements

$$\sigma^2_{ij}(t') = \iint r'_i r'_j P(r'_x, r'_y; t')\, dr'_i\, dr'_j, \tag{2}$$

and $P(r'_x, r'_y; t')$ is the probability distribution function (pdf) of the anomalous relative particle displacements $\mathbf{r}' = (r'_x, r'_y)$. The anomalous relative position displacements were calculated for each drifter as $\mathbf{r}'(t') = \mathbf{r}(t') - \mathbf{R}(t')$, where $\mathbf{R}(t')$ is the mean spatial displacement of all drifters for the time step t' and all arbitrary t'_0 (Spydell et al. 2007; Brown et al. 2009). The pdf of the anomalous relative position displacements $P(r'_x, r'_y; t')$ represents the ensemble average evolution of the drifters from a common initial point source.

To evaluate the fate of material outside the surf zone, only drifter positions recorded seaward of the surf zone ($x > L_x$) for durations of at least 60 s were evaluated. The probability distributions of the anomalous displacements for $t' = 2$ s, $P(r'_x, r'_y; t' = 2\,\text{s})$, were relatively centered about zero in the cross-shore direction, indicating an equal amount of drifters moved seaward and shoreward (Fig. 6). The $P(r'_x, r'_y; t' = 2\,\text{s})$ were similar for all drifter deployments regardless of the drifter pattern observed (Fig. 6), were slightly negatively skewed (skewness of -0.24 to -0.05), and had kurtosis values ranging from 2.8 to 4.9, suggesting that the distributions were basically Gaussian (kurtosis = 3). This is consistent with the findings of Spydell et al. (2009), which demonstrated that drifter displacement pdfs were likely Gaussian for very short time steps ($t' < 15$ s) using a Kolmogorov–Smirnov test. Therefore, there was a relatively equal chance that a drifter outside of the surf zone would move seaward or shoreward, which

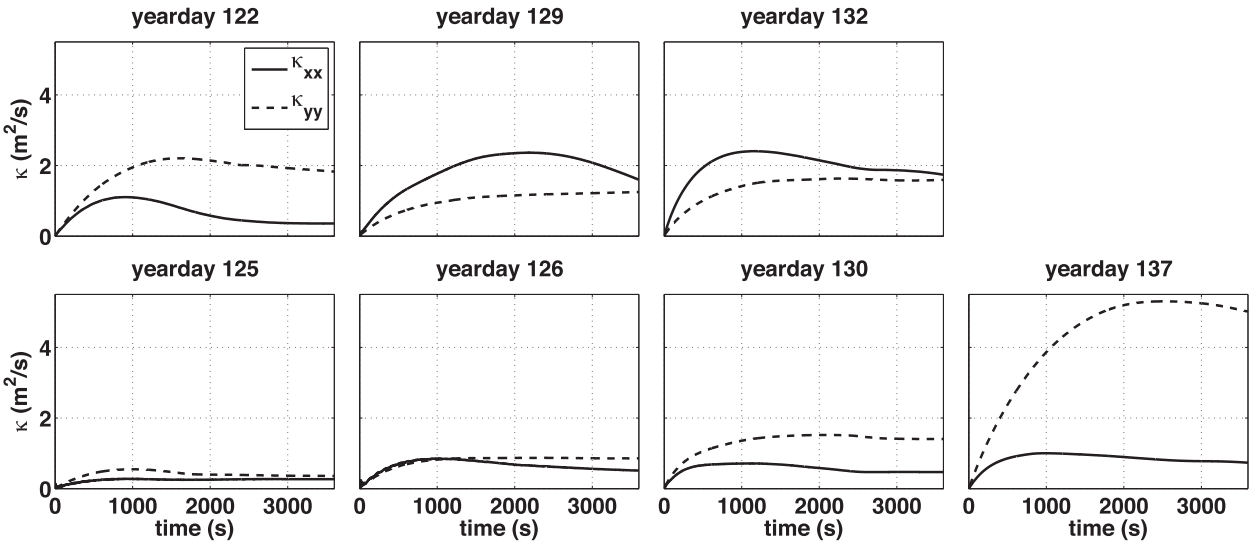

FIG. 7. Absolute diffusivity (one particle) statistics for the cross-shore (κ_{xx}, solid) and alongshore (κ_{yy}, dashed) for drifter positions recorded outside the surf zone for (top) drifter deployments exhibiting the locally contained cross-shore exchange drifter pattern on yeardays 122, 129, and 132 and (bottom) drifter deployments exhibiting the cross-shore and alongshore exchange drifter pattern on yeardays 125, 126, 130, and 137.

supports the qualitative observations that the drifters did not leave the nearshore system (Figs. 4, 5).

The cross-shore absolute diffusivities κ_{xx} [Eq. (1)] outside the surf zone showed similar behavior for all current patterns, with κ_{xx} rising to a peak and then decreasing to an asymptotic value (Fig. 7). The time to reach the peak κ_{xx} was generally 900 to 1140 s, with the exception of yearday 129, which occurred at 2160 s. In general, the values of κ_{xx} were greater during observations of locally contained cross-shore exchange, with peak values of κ_{xx} of 1.11 to 2.41 $m^2 s^{-1}$ and asymptotic values of κ_{xx}^{∞} of 0.36 to 1.74 $m^2 s^{-1}$. During observations of alongshore and cross-shore exchange, the difference in the peak and asymptotic values of κ_{xx} were relatively small, with peak values of κ_{xx} of 0.28 to 1.00 $m^2 s^{-1}$ and asymptotic values of κ_{xx}^{∞} of 0.27 to 0.73 $m^2 s^{-1}$. This indicates that there was more cross-shore mixing outside the surf zone because of the stronger surfzone rip current flows that occurred during the times of locally contained cross-shore exchange. It also suggests that the material being pulled back into the surf zone during strong rip current conditions will be well mixed.

The alongshore absolute diffusivities κ_{yy} [Eq. (1)] outside the surf zone increased approximately monotonically to an asymptotic level κ_{yy}^{∞} for all drifter releases (Fig. 7). During observations of locally contained cross-shore exchange, κ_{xx}^{∞} was greater than κ_{yy}^{∞}, with the exception of yearday 122, because of the predominant movement and spreading of the drifters in the cross-shore direction while remaining within a relatively narrow alongshore region. However, during observations exhibiting cross-shore and alongshore exchange, values of κ_{yy}^{∞} were greater than κ_{xx}^{∞} due to the drifters spreading more in the alongshore direction, and there being less cross-shore mixing due to weaker rip current conditions.

The behavior of κ_{xx} rising to a peak and decreasing to an asymptotic value observed outside the surf zone may be a result of the diffusion not being unbounded (Spydell and Feddersen 2012). Inside the surf zone, this behavior was attributed to the presence of a shoreline boundary (Spydell and Feddersen 2012); however, a nonmonotonic κ_{xx} could also be due to weaker diffusivity seaward of the surf zone. This supports the findings that, in general, the asymptotic values of diffusivity obtained outside the surf zone (κ_{xx}^{∞} = 0.27 to 1.74 $m^2 s^{-1}$; κ_{yy}^{∞} = 0.36 to 5.01 $m^2 s^{-1}$) were smaller than those measured in previous experiments inside the surf zone (κ_{xx}^{∞} = 0.50 to 2.50 $m^2 s^{-1}$; κ_{yy}^{∞} = 2.00 to 12.60 $m^2 s^{-1}$) (Spydell et al. 2007; Brown et al. 2009; Spydell et al. 2009). Additionally, the time to approach κ_{xx}^{∞} and κ_{yy}^{∞} is longer outside the surf zone (>1000 s) compared to κ_{xx}^{∞} and κ_{yy}^{∞} of less than 1000 s found in previous work inside the surf zone (Brown et al. 2009; Spydell et al. 2009), indicating differences in Lagrangian time scales inside and outside the surf zone (Spydell and Feddersen 2012). For all drifter deployments, the absolute diffusivities lacked oscillations, which were observed previously inside the surf zone (Brown et al. 2009), indicating different eddy processes with different spatial and time

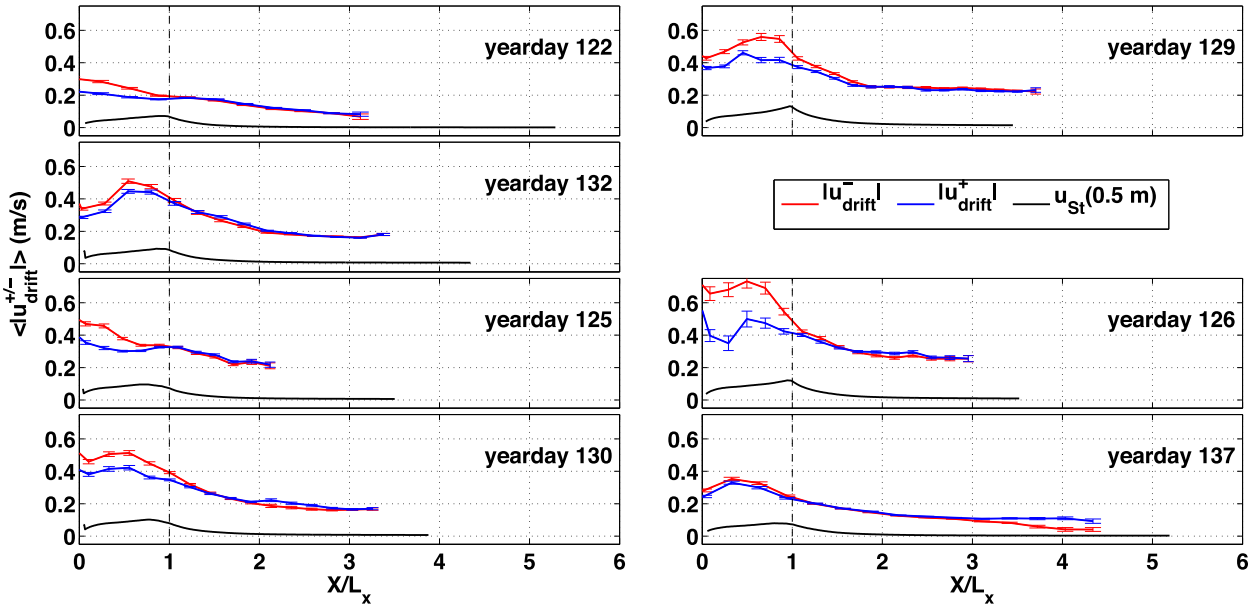

FIG. 8. Mean drifter cross-shore velocity magnitude $\langle|u^{+/-}_{\text{drift}}|\rangle$ as a function of cross-shore distance from the shoreline relative to the surfzone width X/L_x for each drifter deployment, where shoreward velocities $\langle|u^{-}_{\text{drift}}|\rangle$ are shown in red and seaward velocities $\langle|u^{+}_{\text{drift}}|\rangle$ are shown in blue, and error bars representing the 95% confidence intervals are shown. Black line represents the theoretical estimate of the Stokes drift averaged over the upper 0.5 m of the water column $u_{\text{St}}(0.5\,\text{m})$, which corresponds to the depth of the surface drifters. Rows 1 and 2 show drifter deployments exhibiting the locally contained cross-shore exchange drifter pattern on yeardays 122, 129, and 132, and rows 3 and 4 show drifter deployments exhibiting the cross-shore and alongshore exchange drifter pattern on yeardays 125, 126, 130, and 137.

scales are responsible for mixing material on the inner shelf.

c. *Cross-shore variation in drifter cross-shore velocity magnitude*

The behavior of the drifters moving seaward u^{+}_{drift} and shoreward u^{-}_{drift} was evaluated by examining the drifter cross-shore velocity magnitude $|u^{+/-}_{\text{drift}}|$ as a function of cross-shore location X/L_x. The study area was divided into 25-m bins in the cross-shore direction, and the seaward- ($u_{\text{drift}} \geq 0\,\text{m s}^{-1}$) and shoreward-moving ($u_{\text{drift}} < 0\,\text{m s}^{-1}$) drifters in each cross-shore bin were averaged separately over the entire alongshore distance, denoted as $\langle|u^{+}_{\text{drift}}|\rangle$ and $\langle|u^{-}_{\text{drift}}|\rangle$ (Fig. 8). The $\langle|u^{+/-}_{\text{drift}}|\rangle$ were similar for all drifter deployments; that is, the drifter velocities measured for the locally contained cross-shore exchange drifter pattern were not necessarily greater or less than those measured for the cross-shore and alongshore exchange drifter pattern.

Outside the surf zone, the mean velocity magnitude of the seaward- and shoreward-moving drifters was nearly equal: $\langle|u^{+}_{\text{drift}}|\rangle \approx \langle|u^{-}_{\text{drift}}|\rangle$. The $\langle|u^{+/-}_{\text{drift}}|\rangle$ tended to decrease within the distance of one surfzone width offshore of the surf zone (i.e., from $X/L_x = 1$ to $X/L_x = 2$), and $\langle|u^{+/-}_{\text{drift}}|\rangle$ was relatively constant offshore of $X > 2L_x$ for all drifter deployments (Fig. 8). The average change in $\langle|u^{+/-}_{\text{drift}}|\rangle$ offshore of the surf zone was $\Delta\langle|u^{+/-}_{\text{drift}}|\rangle = \langle|u^{+/-}_{\text{drift}}(1L_x)|\rangle - \langle|u^{+/-}_{\text{drift}}(2L_x)|\rangle \approx 0.12\,\text{m s}^{-1}$, including seaward and shoreward drifter velocities. At the edge of the surf zone, the shoreward drifter velocities were greater than the seaward component, possibly because of the surfing of the shoreward-moving drifters in the breaking waves. Inside the surf zone, the shoreward drifter velocities over the shoals were larger than the seaward drifter velocities in the rip channel because of continuity (MacMahan et al. 2004).

These results show that the drifters exiting the surf zone, as a result of rip current pulses, and moving seaward had large velocities at the edge of the surf zone, which subsequently decreased as they continued to move seaward, resulting in a deceleration of the drifters as they exited the surf zone. The drifters outside the surf zone moving shoreward demonstrated an increase in the velocity magnitude as they approached the edge of the surf zone. Therefore, the shoreward-moving drifters were actually accelerating as they reentered the surf zone over shoals.

The $\langle|u^{+/-}_{\text{drift}}|\rangle$ measurements outside the surf zone are compared to theoretical estimates of the Stokes drift near the surface, as a function of cross-shore location (Fig. 8). The Stokes drift $u_{\text{St}}(z)$ was computed as

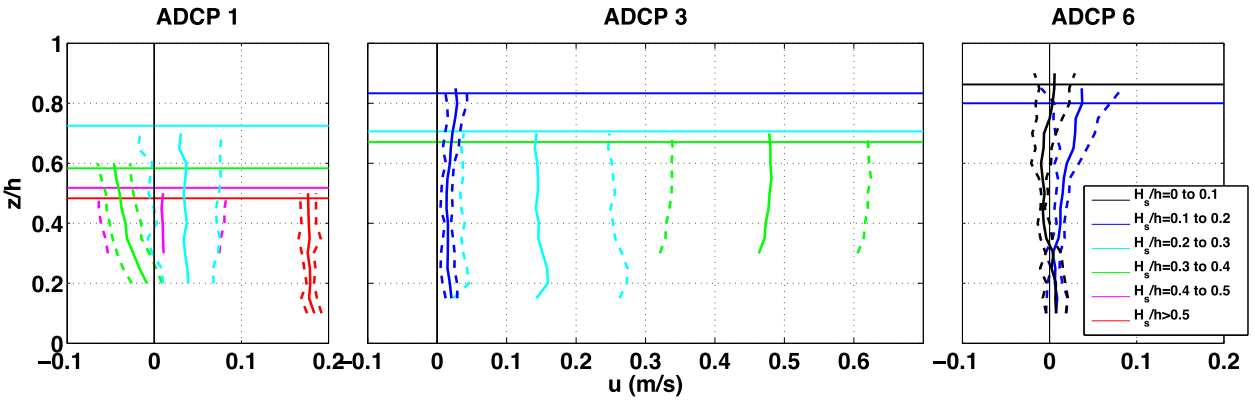

FIG. 9. Average current profiles of 3-h mean vertical profiles, centered around low tide, of cross-shore Eulerian currents for the H_s/h ranges given in the legend, measured at (left) ADCP 1 located at the surfzone boundary over a shoal, (middle) ADCP 3 located at the surfzone boundary in the rip channel, and (right) ADCP 6 located outside the surf zone and offshore of the rip channel. Solid and dashed profiles represent the average ± one standard deviation of the current profiles in each H_s/h range, and only the measurements below the wave trough are shown, where the colored horizontal lines represent the approximate relative depth of the wave trough for the given H_s/h range. Note the variable velocity scales, where positive cross-shore velocity is seaward.

$$u_{\mathrm{St}}(z) = \frac{H_s^2 \omega k}{16} \frac{\cosh[2k(z+h)]}{\sinh^2 kh} \cos\theta_w, \qquad (3)$$

where ω is the wave frequency, k is the wavenumber, and θ_w is the mean wave direction (Stokes 1847; LeBlond and Mysak 1978). Then $u_{\mathrm{St}}(z)$ was averaged over the upper 0.5 m of the water column corresponding to the depth of the surface drifters, indicated as $u_{\mathrm{St}}(0.5\,\mathrm{m})$. The cross-shore variation of $u_{\mathrm{St}}(0.5\,\mathrm{m})$ was computed using Eq. (3) and wave parameters measured in 13-m water depth and shoaled to the shoreline using the alongshore-averaged, cross-shore beach profile adjusted for tides, as described in section 2a. In all cases, $\langle|u^-_{\mathrm{drift}}|\rangle$ was greater than the $u_{\mathrm{St}}(0.5\,\mathrm{m})$ estimates as a function of cross-shore location (Fig. 8). Therefore, the return of the drifters shoreward was not solely due to the net onshore Stokes drift due to waves.

4. Eulerian observations

a. 3D variations of the rip current flow

The Eulerian measurements made by the array of ADCPs show differences in the magnitude and vertical structure of the cross-shore flows between the ADCP on a shoal (ADCP 1) and the ADCPs in the rip channel (ADCPs 3 and 6). To examine these differences, the cross-shore velocities measured during low tides, when rip current flows are known to be strongest (MacMahan et al. 2006), were evaluated. While limiting the Eulerian data analysis to low tides makes the results less general, it better allows for the rip current behavior to be examined. For each ADCP, current profiles from a 3-h window centered about low tide were evaluated. The time series were divided into 15-min segments and the local wave height during that time was computed. Data above the wave trough, computed as the 15-min mean water depth minus the wave amplitude ($H_s/2$), were set to zero. Then, 3-h mean vertical current profiles were computed and interpolated to a depth-relative reference frame z/h using the 3-h mean water depth, where $z/h = 0$ is at the seabed and $z/h = 1$ is at the mean sea surface. These mean current profiles were then sorted by local H_s/h and averaged, as shown in Fig. 9. Averaging Eulerian current profiles includes measurements between the wave trough and crest, and therefore for $z/h > 1$. The approximate relative depth of the wave trough for each H_s/h range is shown in Fig. 9.

In general, at a given ADCP location, the magnitude of the cross-shore velocity was greater for larger H_s/h, representative of larger waves and/or lower tides. These Eulerian measurements support the Lagrangian drifter observations of decreasing $\langle|u^{+/-}_{\mathrm{drift}}|\rangle$ with increasing distance offshore, where smaller H_s/h are indicative of measurements farther outside of wave breaking. Additionally, for a given H_s/h range, the magnitude of the seaward cross-shore velocities were greatest in the center of the rip channel near the edge of the surf zone at ADCP 3 and were smallest over the shoals at ADCPs 1 and 5 (Fig. 9).

The measured Eulerian cross-shore velocity profiles revealed more variation over the vertical, particularly near the surface (just below the wave trough), within the rip channel. In the center of the rip channel near the surfzone boundary at ADCP 3, the measured mean rip current velocity profile was surface dominated, with more vertical structure for smaller H_s/h, and was more

depth uniform for larger H_s/h, representative of times when it was near the onset of wave breaking and just outside the surf zone (Fig. 9). Well offshore of the surf zone (approximately 100 m), at ADCP 6, the measured seaward rip current flow was also surface dominated, demonstrating the cross-shore extent of the rip current flows that exit the surf zone. These results support the laboratory measurements of Haas and Svendsen (2002) and reveal that the vertical profile of the rip current velocity is strongest and depth uniform as it exits the surf zone and then becomes surface dominated and decays in magnitude with distance offshore. The cross-shore velocity profiles measured by ADCP 1 over a shoal were vertically uniform below the wave trough for all values of H_s/h and were even onshore at times for $H_s/h > 0.4$ when they were inside the surf zone.

b. Depth-averaged flows

Observed hourly mean cross-shore velocity profiles measured by each ADCP throughout the entire experiment were used to estimate the depth-averaged Eulerian flows below the wave trough $\overline{u}_E$. The velocity was assumed uniform between the lowest measurement (generally 0.5 m above the seabed) and the seabed (Lentz et al. 2008), and $\overline{u}_E$ was estimated using trapezoidal integration and averaging over the depth below the wave trough. Additionally, the depth-averaged Stokes drift $\overline{u}_{\mathrm{St}}$ associated with the surface gravity waves was estimated as

$$\overline{u}_{\mathrm{St}} = \frac{Q_{\mathrm{St}}}{h} = \frac{gh}{16c}\left(\frac{H_s}{h}\right)^2 \cos\theta_w, \tag{4}$$

where Q_{St} is the volume Stokes transport, which is equal to the depth-integrated $u_{\mathrm{St}}(z)$; g is gravitational acceleration; and c is the wave phase speed (Stokes 1847). The depth-averaged velocities $\overline{u}_{\mathrm{St}}$ and $\overline{u}_E$ were normalized by $(16c/gh)$, represented as $\overline{u}_{N,\mathrm{St}}$ and $\overline{u}_{N,E}$, and were bin averaged as a function of H_s/h, as shown in Fig. 10. Values of the theoretical normalized $\overline{u}_{N,\mathrm{St}}$ computed using Eq. (4) are indicated by a solid black line in Fig. 10. The location of the onset of wave breaking is defined as $H_s/h > 0.4$ and is shown in Fig. 10 (vertical dotted black line) to describe the observations as being either inside or outside of the surf zone.

In general, field observations of $\overline{u}_{N,E}$ increased with increasing H_s/h, associated with increasing wave heights and/or lower tides. For small waves and/or higher tides ($H_s/h < 0.2$), measured $\overline{u}_{N,E}$ was approximately equal to $\overline{u}_{N,\mathrm{St}}$ (Fig. 10, solid black line). This is consistent with observations on the inner shelf by Lentz et al. (2008) and indicates zero net Lagrangian cross-shore transport well outside of the surf zone. A transition in $\overline{u}_{N,E}$ exists

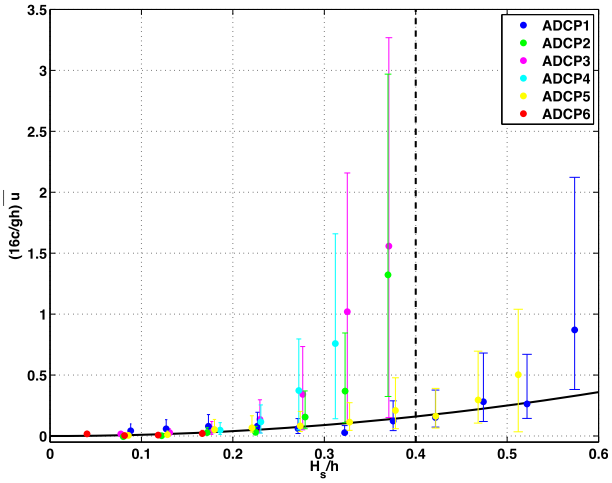

FIG. 10. Normalized, depth-averaged below the wave trough, cross-shore Eulerian currents $\overline{u}_{N,E}$, with error bars representing the 95% confidence intervals, measured at each ADCP and bin averaged by H_s/h, where ADCPs 2, 3, and 4 were located at the surfzone boundary inside the rip channel, ADCPs 1 and 5 were located at the surfzone boundary over shoals, and ADCP 6 was located outside the surf zone offshore of the rip channel. Solid black line represents theoretical Stokes drift magnitude $\overline{u}_{N,\mathrm{St}}$ that balances $\overline{u}_{N,E}$ according to Lentz et al. (2008). Vertical dashed black line represents the location of wave breaking, where $H_s/h < 0.4$ is outside of the surf zone.

approaching the surfzone boundary ($0.2 < H_s/h < 0.4$), where for a given range of H_s/h, the magnitude of $\overline{u}_{N,E}$ was dependent upon the alongshore location of the ADCP (i.e., within the rip channel or not). The $\overline{u}_{N,E}$ measured by ADCPs 1 and 5 (Fig. 10, blue and yellow) were small and directed offshore and remained consistent with Eq. (4) and Lentz et al. (2008). However, this is attributed to ADCPs 1 and 5 being located at the borderline of the rip current width, yet not directly over the shoals, and therefore the measured velocities were typically small and directed both offshore and onshore, such that the bin-averaged value for a given H_s/h was small and not representative of strong offshore rip current flows nor onshore flows. Also, because ADCPs 1 and 5 were not located directly over shoals and the measured values of $\overline{u}_{N,E}$ are not directed shoreward, these measurements do not match the observations of the shoreward-moving drifters over the shoals. However, $\overline{u}_{N,E}$ measured within the rip channel by ADCPs 2, 3, and 4 (Fig. 10, green, magenta, and cyan) tended to exceed the theoretical Stokes drift transport $\overline{u}_{N,\mathrm{St}}$ [Eq. (4)]. This indicates a deviation from the results of Lentz et al. (2008) near the surfzone boundary. Additionally, there is a greater imbalance (larger offshore transport) at the surfzone boundary that decreases with distance offshore (decreasing H_s/h), consistent with the drifter observations. The consistency in the measurements by

ADCPs 2, 3, and 4 demonstrates that each ADCP was measuring seaward rip current flows. Inside of the surf zone ($H_s/h > 0.4$), no measurements of $\overline{u}_{N,E}$ in the rip currents were obtained.

5. Discussion

a. *Comparison to cross-shore exchange on alongshore homogeneous beaches*

The shoreward-moving Lagrangian drifters on the inner shelf of the rip-channeled beach were observed to accelerate as they approached the surfzone boundary and reentered the surf zone over shoals. These results differ from those of Ohlmann et al. (2012), who observed a tendency for drifters released on the inner shelf of alongshore homogeneous beaches in Santa Barbara and Huntington Beach, California, to decelerate as they moved shoreward. This was explained using the theoretical undertow model of Lentz et al. (2008). Near the surfzone boundary ($h < 3$ m), the modeled $u_E(z)$ was surface intensified and directed offshore and $u_{St}(z)$ was more vertically uniform, resulting in a net offshore Lagrangian velocity at the surface. This imbalance explained approximately half of the observed drifter decelerations. The remainder of the decelerations was attributed to the coastal boundary condition, where onshore winds create a shoreward-moving surface layer resulting in an overturning circulation near the coast and a seaward-moving lower layer, with the bottoms of the drifters potentially extending into this lower layer. Other suggested contributors to the drifter decelerations included the existence of a temperature gradient between the warmer, near-surface surfzone water and that just outside the surf zone, resulting in a density barrier preventing onshore transport into the surf zone as well as transient rip currents observed at one field site. The mechanism for the onshore motion of the drifters could not be discerned by Ohlmann et al. (2012). The substantial differences in the behavior of shoreward-moving drifters on the inner shelf as they approach the surfzone boundary observed on the rip-channeled beach here and by Ohlmann et al. (2012) on an alongshore homogeneous beach suggests that the surfzone rip current circulations may contribute to the acceleration of shoreward-moving drifters into the surf zone over the shoals on the rip-channeled beach.

Cross-shore exchange was also examined by Hally-Rosendahl et al. (2014) on an alongshore homogeneous beach in Imperial Beach, California, using dye and water temperature as tracers. Dye released continuously near the shoreline in an alongshore current was well mixed within the surf zone. Measurements of warm, dye-rich water were observed on the inner shelf and found to be alongshore patchy, which was attributed to local cross-shore advection from the surf zone via transient rip currents, as opposed to exchange due to the imbalance of Stokes drift and wave-driven Eulerian undertow at the surfzone boundary. The dye transported seaward to the inner shelf was determined to have been recycled back into the surf zone, based on the significant levels of dye measured alongshore within the surf zone 8 h after the end of the dye release. These results contrast with the observations of cross-shore exchange by Ohlmann et al. (2012) for different alongshore homogeneous beaches and warrants additional investigation into the mechanisms limiting onshore transport observed by Ohlmann et al. (2012).

The similarities of cross-shore exchange measured on the rip-channeled beach and that measured by Hally-Rosendahl et al. (2014) on an alongshore homogeneous beach with transient rip currents suggests that surfzone vortices associated with rip current dynamics can be a controlling factor of cross-shore exchange. MacMahan et al. (2010b) concluded that VLF vortical motions can occur on any beach because of the modulation of directionally spread incident short waves. Therefore, the observations of cross-shore exchange associated with bathymetrically controlled rip currents described in this work can be used to evaluate cross-shore exchange on beaches without bathymetrically controlled rip currents but where VLF surfzone motions are observed.

b. *Mass balance controlling cross-shore exchange on a rip-channeled beach*

The combination of these rip current flow observations on the inner shelf with previous rip current circulation observations within the surf zone increase our understanding of cross-shore exchange on a rip-channeled beach. Observations of Lagrangian drifters on this same beach by MacMahan et al. (2010a) revealed that rip currents are large-scale vortices predominantly contained within the surf zone, with only episodic exits offshore. The rip current exchange on the rip-channeled beach was driven by VLF rip current pulsations forced by wave groups with $O(10)$ min time scales (Reniers et al. 2009, 2010). Reniers et al. (2009) found that the onshore Stokes drift was responsible for limiting the number of surfzone exits. However, both the Lagrangian drifter observations and the depth-averaged cross-shore Eulerian measurements obtained on the inner shelf indicate that Stokes transport is not solely responsible for the shoreward transport in the nearshore and across the surfzone boundary on the rip-channeled beach. However, a net offshore transport does not exist because the drifter observations on the inner shelf show

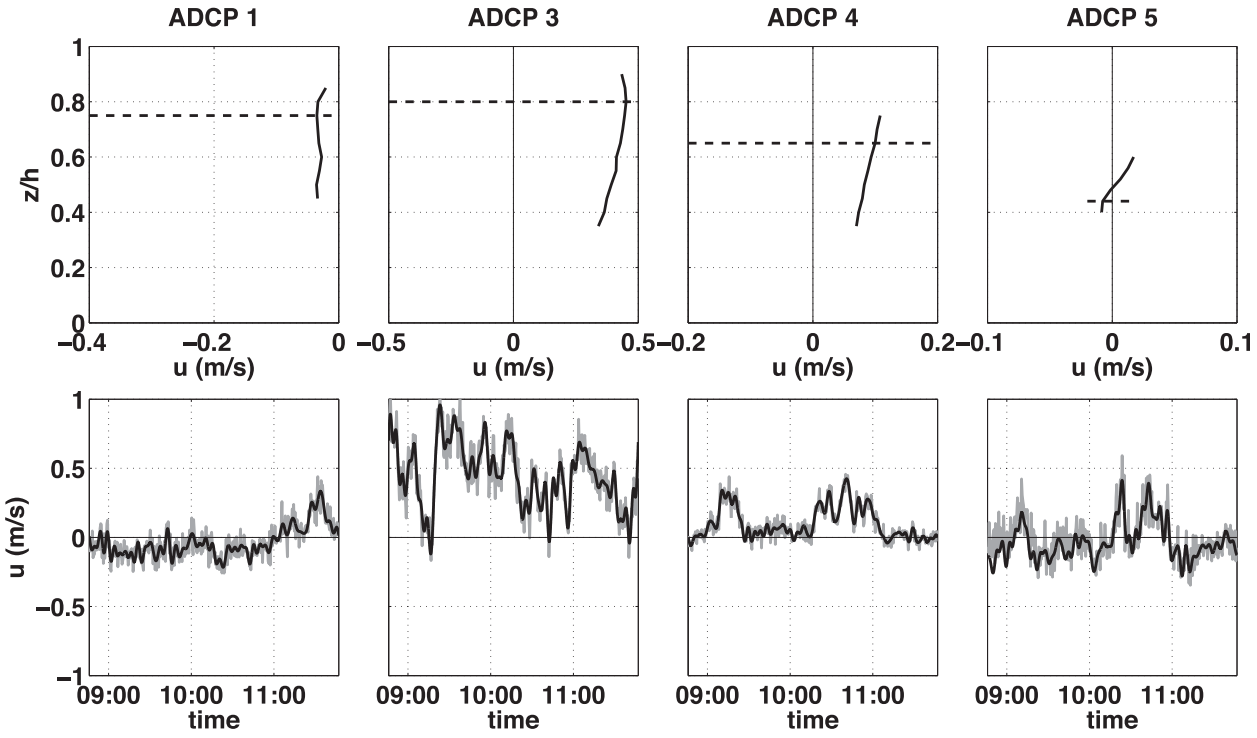

FIG. 11. Eulerian velocity measurements at each ADCP (columns) during the drifter deployment on yearday 132, showing (top) the depth-relative mean cross-shore velocity vertical profile below the wave trough averaged over the duration of the drifter deployment and (bottom) the 30-s-averaged near-surface cross-shore velocity (gray) and low-pass filtered ($f < 0.004$ Hz) near-surface cross-shore velocity (black), representing VLF rip current pulsations, where ADCPs 3 and 4 were located at the surfzone boundary inside the rip channel. The horizontal dashed lines in the top plots represent the relative depth 0.2 m below the wave trough of the near-surface cross-shore velocities shown in the bottom plots. Note the variable velocity scales in the top plots, where positive cross-shore velocity is seaward.

that no drifters completely left the nearshore system. The seaward and shoreward drifter velocity magnitudes were relatively equal outside the surf zone (Fig. 8), implying there was no net Lagrangian mass transport. These results suggest that a recirculation exists across the surfzone boundary, and as material is transported offshore by rip current pulsations, some factor besides Stokes transport must be responsible for pulling material shoreward on the inner shelf and into the surf zone.

It is hypothesized that a mass balance exists on the rip-channeled beach, where the surfzone rip current circulations both eject material offshore in the rip channels as VLF pulses and pull material back into the surf zone over shoals. The vertical structure of the mean Eulerian cross-shore flows measured by the ADCPs during the drifter deployment on yearday 132 (excluding ADCP 2, which was inoperative this day) is shown in Fig. 11 (top row). The mean profiles show offshore flows, which were strongest just below the wave trough and decreased with depth, measured inside the rip channel (ADCPs 3 and 4), and onshore flows, which were vertically uniform below the wave trough, measured by ADCPs 1 and 5, where the magnitude of the measured onshore flows were a fraction of the magnitude of the measured offshore rip current flows. The presence of low-frequency motions was examined in the near-surface cross-shore velocity measured by each ADCP. The near-surface velocity measurements were examined at a relative depth 0.2-m below the depth corresponding to the lowest wave trough measured during the drifter deployment (i.e., the wave trough associated with the largest wave) in order to eliminate any variability due to the moving sea surface (relative depth of velocity measurement shown by horizontal dashed line in Fig. 11, top row). Infragravity motions are shown by a 30-s average of the cross-shore velocity, and the presence of VLF pulses was examined by low-pass filtering ($f < 0.004$ Hz) the near-surface cross-shore velocity measured by the ADCPs (Fig. 11, bottom row). Oscillations were present in the low-pass filtered offshore surface rip current velocity (ADCP 3 and 4) at the VLF time scale with relatively large magnitudes (0.5 to 1.0 m s^{-1}) that represent the VLF rip current pulsations responsible for the rip current exits. Additionally, VLF oscillations of smaller magnitude (0.1 to 0.2 m s^{-1}) were present in the onshore surface velocities over the shoals. These results demonstrate

the VLF pulsating nature of the seaward rip current flows as well as the shoreward flows reentering the surf zone.

6. Summary and conclusions

Cross-shore exchange on a rip-channeled beach at Sand City, California, was examined using an extensive set of Lagrangian and Eulerian field measurements of surf zone and inner shelf rip current flows. The results revealed differences in cross-shore transport from that measured on the inner shelf of alongshore homogeneous beaches and provides new insights into cross-shore exchange on a rip-channeled beach. Position-tracking surface drifters released on the inner shelf were observed to move seaward because of the rip current pulses and then return shoreward in an arcing pattern, reentering the surf zone over shoals. Two drifter patterns were observed: 1) locally contained cross-shore exchange, where the drifters moved seaward and returned sharply back shoreward a short alongshore distance from where they exited (Fig. 4), and 2) cross-shore and alongshore exchange, where the drifters moved seaward and traveled farther in the alongshore direction as they gradually moved shoreward (Fig. 5). The cross-shore extent of the drifters was typically one to two surfzone widths L_x beyond the surfzone boundary.

On the inner shelf of the rip-channeled beach, the rate of spreading and mixing ($\kappa_{xx}^{\infty} = 0.27$ to $1.74\,\mathrm{m^2\,s^{-1}}$; $\kappa_{yy}^{\infty} = 0.36$ to $5.01\,\mathrm{m^2\,s^{-1}}$) was slower than that measured inside the surf zone during previous studies, suggesting there is less lateral shear in the flow field outside the surf zone. In general, the values of κ_{xx} were greater during observations of locally contained cross-shore exchange, indicating more cross-shore mixing outside the surf zone because of the stronger rip current flows. The probability distributions of the drifter cross-shore anomalous relative displacements outside the surf zone were basically Gaussian, indicating there was a relatively equal chance that a drifter anywhere on the inner shelf would move seaward or shoreward, consistent with the qualitative observations that no drifters left the nearshore system. The seaward- and shoreward-moving cross-shore drifter velocities were approximately equal in magnitude as a function of cross-shore location, resulting in a total Lagrangian velocity of approximately zero. The seaward-moving drifters were observed to decelerate after exiting the surf zone through rip channels, while the shoreward-moving drifters were observed to accelerate as they reentered the surf zone over shoals. Near the surfzone boundary, the depth-averaged Eulerian flows $\overline{u}_{N,E}$ measured in the rip channel were largest near the edge of the surf zone, consistent with the drifter observations, and were greater than the depth-averaged theoretical Stokes drift $\overline{u}_{N,\mathrm{St}}$. Additionally, the velocity magnitude of the shoreward-moving drifters outside the surf zone was greater than the near-surface theoretical Stokes drift.

The rip current flow observations on the inner shelf combined with previous surf zone rip current observations contribute to the overall understanding of how material is exchanged and conserved within the nearshore region on a rip-channeled beach. Short waves propagating over the variable surfzone bathymetry drive spatial variations in the wave groups, which force VLF motions and rip current circulations inside the surf zone that episodically expel material offshore through the rip channels and appear to pull material back onshore. Interestingly, no material appears to be completely removed from the nearshore system on the rip-channeled beach.

Acknowledgments. This work was supported by the National Science Foundation (NSF OCE-0926750), and the instrumentation used during the field work was funded by the Office of Naval Research (ONR DURIP N0001409WR20268). J. Brown was supported by the Department of Defense through the National Defense Science and Engineering Graduate (NDSEG) Fellowship and by NSF OCE-0926750. We thank the many people who assisted in collecting the field data: Edie Gallagher, Keith Wyckoff, Ron Cowen, Bill Swick, Ian Smithgall, and Clement Gandon. We would also like to thank our reviewers and Falk Feddersen for their comments and contribution in improving this manuscript.

REFERENCES

Anderson, D. M., 2009: Approaches to monitoring, control and management of harmful algae blooms (HABs). *Ocean Coastal Manage.,* **52,** 342–347, doi:10.1016/j.ocecoaman.2009.04.006.

Boehm, A., B. Sanders, and C. Winant, 2002: Cross-shore transport at Huntington Beach. Implications for the fate of sewage discharged through an offshore ocean outfall. *Environ. Sci. Technol.,* **36,** 1899–1906, doi:10.1021/es0111986.

Bowen, A. J., 1969: Rip currents: 1. Theoretical investigations. *J. Geophys. Res.,* **74,** 5467–5478, doi:10.1029/JC074i023p05467.

Brander, R. W., and A. D. Short, 2001: Flow kinematics of low-energy rip current systems. *J. Coastal Res.,* **17,** 468–481. [Available online at http://www.jstor.org/stable/4300197.]

Brown, J. W., J. H. MacMahan, A. J. H. M. Reniers, and E. B. Thornton, 2009: Surfzone diffusivity on a rip-channeled beach. *J. Geophys. Res.,* **114,** C11015, doi:10.1029/2008JC005158.

Clark, D. B., S. Elgar, and B. Raubenheimer, 2012: Vorticity generation by short-crested wave breaking. *Geophys. Res. Lett.,* **39,** L24604, doi:10.1029/2012GL054034.

Dean, R. G., and R. A. Dalrymple, 1984: *Water Wave Mechanics for Engineers and Scientists.* Prentice-Hall, 353 pp.

Garcez Faria, A. F., E. B. Thornton, T. C. Lippmann, and T. P. Stanton, 2000: Undertow over a barred beach. *J. Geophys. Res.,* **105,** 16 999–17 010, doi:10.1029/2000JC900084.

Grant, S. B., J. H. Kim, B. H. Jones, S. A. Jenkins, J. Wasyl, and C. Cudaback, 2005: Surfzone entrainment, along-shore transport, and human health implications of pollution from tidal outlets. *J. Geophys. Res.,* **110,** C10025, doi:10.1029/2004JC002401.

Haas, K. A., and I. A. Svendsen, 2002: Laboratory measurements of the vertical structure of rip currents. *J. Geophys. Res.,* **107** (C5), doi:10.1029/2001JC000911.

Haines, J. W., and A. H. Sallenger Jr., 1994: Vertical structure of mean cross-shore currents across a barred surfzone. *J. Geophys. Res.,* **99,** 14 223–14 242, doi:10.1029/94JC00427.

Hally-Rosendahl, K., F. Feddersen, and R. T. Guza, 2014: Cross-shore tracer exchange between the surfzone and inner-shelf. *J. Geophys. Res. Oceans,* **119,** 4367–4388, doi:10.1002/2013JC009722.

Hasselmann, K., 1970: Wave-driven inertial oscillations. *Geophys. Fluid Dyn.,* **1,** 463–502, doi:10.1080/03091927009365783.

Hendrickson, J., and J. H. MacMahan, 2009: Diurnal sea breeze effects on inner-shelf cross-shore exchange. *Cont. Shelf Res.,* **29,** 2195–2206, doi:10.1016/j.csr.2009.08.011.

Inman, D. L., and B. M. Brush, 1973: Coastal challenge. *Science,* **181,** 20–32, doi:10.1126/science.181.4094.20.

Johnson, D., and C. Pattiaratchi, 2004: Transient rip currents and nearshore circulation on a swell-dominated beach. *J. Geophys. Res.,* **109,** C02026, doi:10.1029/2003JC001798.

Kirincich, A. R., S. J. Lentz, and J. A. Barth, 2009: Wave-driven inner-shelf motions on the Oregon coast. *J. Phys. Oceanogr.,* **39,** 2942–2956, doi:10.1175/2009JPO4041.1.

Large, W. G., and S. Pond, 1981: Open ocean momentum flux measurements in moderate to strong winds. *J. Phys. Oceanogr.,* **11,** 324–336, doi:10.1175/1520-0485(1981)011<0324:OOMFMI>2.0.CO;2.

LeBlond, P. H., and L. A. Mysak, 1978: *Waves in the Ocean.* Elsevier, 602 pp.

Lentz, S. J., M. Fewings, P. Howd, J. Fredericks, and K. Hathaway, 2008: Observations and a model of undertow over the inner continental shelf. *J. Phys. Oceanogr.,* **38,** 2341–2357, doi:10.1175/2008JPO3986.1.

MacMahan, J. H., 2001: Hydrographic surveying from a personal watercraft. *J. Surv. Eng.,* **127,** 12–24, doi:10.1061/(ASCE)0733-9453(2001)127:1(12).

——, A. J. H. M. Reniers, E. B. Thornton, and T. P. Stanton, 2004: Infragravity rip current pulsations. *J. Geophys. Res.,* **109,** C01033, doi:10.1029/2003JC002068.

——, E. B. Thornton, T. P. Stanton, and A. J. H. M. Reniers, 2005: RIPEX: Observations of a rip current system. *Mar. Geol.,* **218,** 113–134, doi:10.1016/j.margeo.2005.03.019.

——, ——, and A. J. H. M. Reniers, 2006: Rip current review. *Coastal Eng.,* **53,** 191–208, doi:10.1016/j.coastaleng.2005.10.009.

——, J. W. Brown, and E. B. Thornton, 2009: Low-cost handheld global positioning system for measuring surf-zone currents. *J. Coastal Res.,* **25,** 744–754, doi:10.2112/08-1000.1.

——, and Coauthors, 2010a: Mean Lagrangian flow behavior on an open coast rip-channeled beach: A new perspective. *Mar. Geol.,* **268,** 1–15, doi:10.1016/j.margeo.2009.09.011.

——, A. J. H. M. Reniers, and E. B. Thornton, 2010b: Vortical surfzone velocity fluctuations with O(10) min period. *J. Geophys. Res.,* **115,** C06007, doi:10.1029/2009JC005383.

Michel, J., and Coauthors, 2013: Extent and degree of shoreline oiling: Deepwater horizon oil spill, Gulf of Mexico, USA. *PLoS One,* **8,** e65087, doi:10.1371/journal.pone.0065087.

Monismith, S. G., E. A. Cowen, H. M. Nepf, J. Magnaudet, and L. Thais, 2007: Laboratory observations of mean flows under surface gravity waves. *J. Fluid Mech.,* **573,** 131–147, doi:10.1017/S0022112006003594.

Ohlmann, J. C., M. R. Fewings, and C. Melton, 2012: Lagrangian observations of inner-shelf motions in southern California: Can surface waves decelerate shoreward-moving drifters just outside the surfzone? *J. Phys. Oceanogr.,* **42,** 1313–1326, doi:10.1175/JPO-D-11-0142.1.

Putrevu, U., and I. A. Svendsen, 1993: Vertical structure of the undertow outside the surfzone. *J. Geophys. Res.,* **98,** 22 707–22 716, doi:10.1029/93JC02399.

Reniers, A. J. H. M., J. A. Roelvink, and E. B. Thornton, 2004a: Morphodynamic modeling of an embayed beach under wave group forcing. *J. Geophys. Res.,* **109,** C01030, doi:10.1029/2002JC001586.

——, E. B. Thornton, T. P. Stanton, and J. A. Roelvink, 2004b: Vertical flow structure during Sandy Duck: Observations and modeling. *Coastal Eng.,* **51,** 237–260, doi:10.1016/j.coastaleng.2004.02.001.

——, J. H. MacMahan, E. B. Thornton, T. P. Stanton, M. Henriquez, J. W. Brown, J. A. Brown, and E. Gallagher, 2009: Surfzone surface retention on a rip-channeled beach. *J. Geophys. Res.,* **114,** C10010, doi:10.1029/2008JC005153.

——, ——, F. J. Beron-Vera, and M. J. Olascoaga, 2010: Rip-current pulses tied to Lagrangian coherent structures. *Geophys. Res. Lett.,* **37,** L05605, doi:10.1029/2009GL041443.

Schiff, K. C., M. J. Allen, E. Y. Zeng, and S. M. Bay, 2000: Southern California. *Mar. Pollut. Bull.,* **41,** 76–93, doi:10.1016/S0025-326X(00)00103-X.

Shahidul Islam, M. S., and M. Tanaka, 2004: Impacts of pollution on coastal and marine ecosystems including coastal and marine fisheries and approach for management: A review and synthesis. *Mar. Pollut. Bull.,* **48,** 624–649, doi:10.1016/j.marpolbul.2003.12.004.

Shepard, F. P., K. O. Emery, and E. C. LaFond, 1941: Rip currents: A process of geological importance. *J. Geol.,* **49,** 337–369, doi:10.1086/624971.

Smith, J. A., 2006: Wave–current interactions in finite depth. *J. Phys. Oceanogr.,* **36,** 1403–1419, doi:10.1175/JPO2911.1.

——, and J. L. Largier, 1995: Observations of nearshore circulation-rip currents. *J. Geophys. Res.,* **100,** 10 967–10 975, doi:10.1029/95JC00751.

Spydell, M., and F. Feddersen, 2012: A Lagrangian stochastic model of surfzone drifter dispersion. *J. Geophys. Res.,* **117,** C03041, doi:10.1029/2011JC007701.

——, ——, R. Guza, and W. Schmidt, 2007: Observing surf-zone dispersion with drifters. *J. Phys. Oceanogr.,* **37,** 2920–2939, doi:10.1175/2007JPO3580.1.

——, ——, and ——, 2009: Observations of drifter dispersion in the surfzone: The effect of sheared alongshore currents. *J. Geophys. Res.,* **114,** C07028, doi:10.1029/2009JC005328.

Stokes, G. G., 1847: On the theory of oscillatory waves. *Trans. Cambridge Philos. Soc.,* **8,** 441–455.

Svendsen, I. A., 1984: Mass flux and undertow in a surfzone. *Coastal Eng.,* **8,** 347–365, doi:10.1016/0378-3839(84)90030-9.

Taylor, G. I., 1922: Diffusion by continuous movements. *Proc. London Math. Soc.,* **20,** 196–212, doi:10.1112/plms/s2-20.1.196.

Thornton, E. B., and R. T. Guza, 1982: Energy saturation and phase speeds measured on a natural beach. *J. Geophys. Res.,* **87,** 9499–9508, doi:10.1029/JC087iC12p09499.

Xu, Z., and A. J. Bowen, 1994: Wave- and wind-driven flow in water of finite depth. *J. Phys. Oceanogr.,* **24,** 1850–1866, doi:10.1175/1520-0485(1994)024<1850:WAWDFI>2.0.CO;2.